J. Phys. Chem. A **2006,** *110,* 8893−8900 **8893**

Theoretical Investigation of the Mechanisms of Reactions of H_2CN and H_2SiN with NO

Hui-Lung Chen, Ching-Wen Wu, and Jia-Jen Ho*

Department of Chemistry, National Taiwan Normal University, 88, Section 4, Tingchow Road, Taipei 116, Taiwan

Received: January 18, 2006; In Final Form: May 19, 2006

The mechanisms of the reaction of H_2XN (X = C, Si) with NO were studied at the level CCSD(T)/aug-cc-PVTZ//B3LYP/6-31++G(d,p). The results indicate that there are two most favorable reaction pathways in the reaction H_2CN + NO that have similar energy barriers; these two pathways lead to the formation of HCN + HNO (P1) and H_2CO + N_2 (P3), with the calculated barriers 11.1 and 10.2 kcal/mol, respectively, with respect to the reactants (H_2CN + NO). In the reaction H_2SiN + NO the difference of the barriers in these two analogous pathways becomes large, and the preferable pathway shifts to the production of H_2SiO + N_2 (P3s), which has no barrier with respect to the reactants (H_2SiN + NO). A direct reduction of NO into a stable and nontoxic nitrogen molecule with no energy input becomes possible. As a consequence, H_2SiN might be an effective reagent to convert the reactive and toxic NO into a benign gas N_2 in several NO-producing combustion systems. We offer a possible explanation of the differences between H_2CN and H_2SiN toward NO as well as the calculated potential energies for these reactions.

Introduction

Since its first discovery in 1962 by Cochran et al.,[1] the methylene amidogen radical (H_2CN) has been of interest to experimentalists and theoreticians. It was detected in interstellar clouds and was proposed to play a role in extraterrestrial atmospheres.[2−5] This free radical is a key reactive intermediate in the combustion of RDX $(CH_2NNO_2)_3$ and HMX $(CH_2NNO_2)_4$ in their early stages.[6−9] It might be formed directly from the fragmentation of these energetic molecules or indirectly from the decomposition of CH_2NNO_2 (methylene nitramine), the building block of RDX and HMX. This radical is also believed to play a role in the combustion chemistry of hydrocarbon flames containing nitrogen,[10] in the reburning of NO,[11] and in interstellar clouds.[12]

The production of nitrogen oxides via the combustion of fossil fuels attracts great interest because these oxides are considered to be toxic pollutants to the atmosphere. Over the years significant efforts have been undertaken to develop a detailed mechanism of reaction for the selective noncatalytic reduction of nitric oxide by ammonia.[13−17] This process, which was discovered by Lyon[18] in 1972 and is coined thermal DeNO$_x$, is widely used as a practical technique to control NO$_x$. The key reaction in thermal DeNO$_x$ is the reaction between NH_2 and NO, which has two major product channels:

$$NH_2 + NO \leftrightarrow NNH + OH \quad \text{a radical-producing channel}$$

$$NH_2 + NO \leftrightarrow N_2 + H_2O \quad \text{a chain-terminating channel}$$

Although the model proves to be successful in predicting the actual field performance,[19] details of the reaction mechanism remain controversial. Several other studies[20−30] have been conducted involving catalysts to eliminate the production of NO$_x$, but the diversity and complexity of these reaction mechanisms are still unknown. In addition, Hershberger et al.[31−35] have reported several important dynamics and kinetics as well as theoretical studies about the topics of nitrogen-containing compounds such as NCO, NCN, CCO, and HCCO with NO$_x$ reactions. Furthermore, there are several other theoretical studies[36−40] of the mechanisms of the reactions of nitric oxide that occur in an internal-combustion engine, and several experimental studies about the reaction of nitric oxide with organic compounds were reported by Hrabie and Keefer et al.[41,42]

Our purpose in this work was to find possible reactants that might both react with NO to form a stable product such as N_2 that is not harmful to our environment and have possibly a smaller energy barrier. The first portion of this paper focuses on H_2CN as a reactant with NO; we calculated most of the probable reaction pathways and plotted the potential-energy surfaces. We also searched for a possible pathway leading to stable N_2 and performed calculations of the transition barrier. In the second portion we replace H_2CN with H_2SiN and emphasize this pathway of N_2 formation; we found that it was completely barrierless with respect to the reactants.

Computational Methods

Molecular-orbital calculations ‘ab initio’ were conducted with programs in the suite Gaussian 03.[43] The geometrical structures of all reactants, intermediates, transition states, and products were optimized with a hybrid density-functional, B3LYP, method[44,45] with a basis set 6-31++G(d,p). The calculated equilibrium structures (local minima and saddle points) were characterized with calculations of harmonic vibrational wavenumbers at the same level of theory. The correction for zero-point energy (ZPE) was also considered at the level B3LYP/6-31++G(d,p). Calculations of intrinsic reaction coordinates (IRC)[46] were performed at the same level of theory to establish the actual link between the transition state and the intermediates. All the calculation is done on the singlet configuration upon the combination of the reactants. To obtain more reliable

---

* Corresponding author phone: (886)-2-29309085; fax: (886)-2-29324249; e-mail: jjh@ntnu.edu.tw.

10.1021/jp060355q CCC: $33.50

TABLE 1: Geometric Parameters (Bond Lengths and Angles) and Electron Affinities (EA) of the H_2CN Molecule Calculated at Various Levels of Theory and Some Experimental Data Available from the Literature

level of theory	C−N/Å	C−H/Å	∠HCH°	EA/eV[a]
MP2/6-31++G**	1.223	1.092	117.4	0.61
MP2/6-311++G**	1.218	1.097	117.3	0.69
B3LYP/6-31++G**	1.248	1.101	116.9	0.58
B3LYP/6-311++G**	1.242	1.099	116.9	0.60
CCSD(T)/6-31++G**	1.263	1.094	117.5	0.15
CCSD(T)/6-311++G**	1.268	1.101	117.3	0.22
CCSD/aug-cc-PVDZ	1.264	1.106	117.9	0.23
CCSD(T)/aug-cc-PVDZ //B3LYP/6-31++G**				0.36
CCSD(T)/aug-cc-PVTZ //B3LYP/6-31++G**				0.47
experiment	1.247[b]	1.110[b]	116.7[b]	0.511 ± 0.008[c]

[a] Difference between the energies of anion H_2CN^- and the neutral molecule H_2CN. [b] Reference 49. [c] Reference 50.

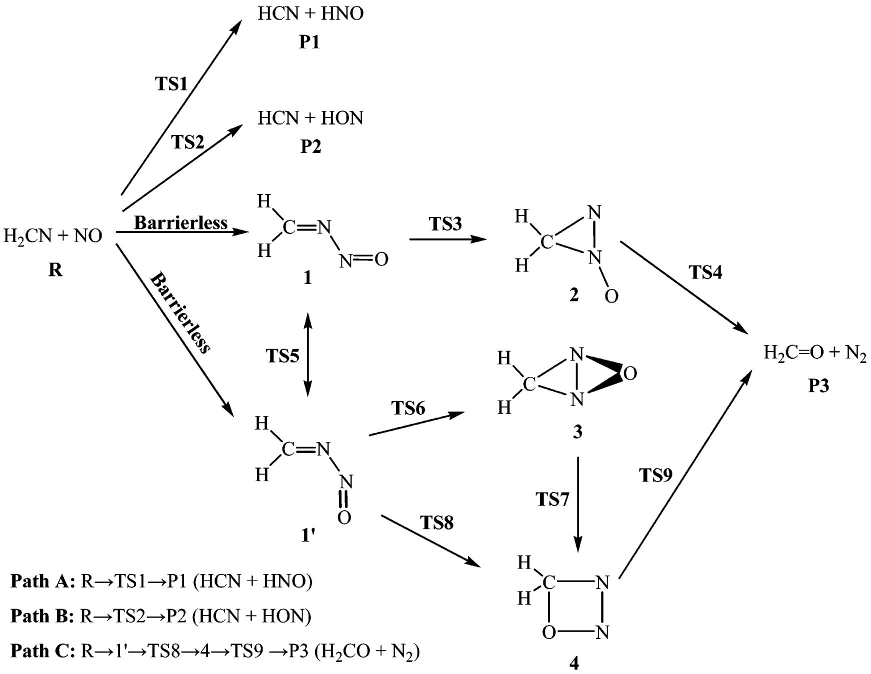

Figure 1. Schematic diagram of proposed pathways for the reaction of H_2CN with NO; three possible channels are characterized as A−C.

energies, we undertook coupled-cluster calculations with single and double excitations and an evaluation by the perturbation theory of triple contributions CCSD(T)[47,48] for those geometries optimized at the level B3LYP/6-31++G(d,p). The highest level of theory attained in this work can thus be denoted CCSD(T)/aug-cc-PVTZ//B3LYP/6-31++G(d,p). Uunless otherwise specified, the CCSD(T) single-point energies are used in the following discussions.

Results and Discussion

In Table 1, we present data for the electron affinities (EA) and geometrical parameters of the H_2CN radical calculated with theory at various levels as well as pertinent experimental data from the literature. The hybrid density-functional B3LYP method with a modest basis set 6-31++G(d,p) predicts the bond lengths in H_2CN to be C−N = 1.248 Å and C−H = 1.101 Å, and the ∠HCH bond angle = 116.9°, in satisfactory agreement with experimental values (1.247, 1.110 Å, and 116.7°, respectively),[49] whereas the calculated B3LYP energy for the electron affinity of H_2CN, 0.58 eV, substantially overestimates the experimental value (0.511 ± 0.008,[50] shown in Table 1). In this regard, we performed a single-point energy calculation at the level CCSD(T)/aug-cc-PVTZ, based on geometries obtained from B3LYP/6-31++G(d,p), to improve this value for H_2CN to 0.47 eV, which is in better agreement than the result obtained at higher level calculation such as CCSD(T)/6-311++G(d,p) (0.22 eV, in Table 1, far off the experimental value of 0.511 ± 0.008). We applied the same method to calculate the ionization energies of the HNO and H_2CO molecules (HNO and H_2CO are among the important products in the title reaction), and the results, $IE_{(HNO)} = 10.15$ eV and $IE_{(H2CO)} = 10.83$ eV, are in satisfactory agreement with the experimental values (10.18 ± 0.01[51] and 10.874 ± 0.002[52] eV, respectively). For this reason, we chose the method CCSD(T)/aug-cc-PVTZ//B3LYP/6-31++G(d,p) to make an energetic calculation for all possible processes in the reaction systems H_2XN + NO, with X = C and Si.

Reaction H_2CN + NO. We classified the investigated reaction into three pathways, **A**−**C**, corresponding to three possible product channels, as depicted in Figure 1. The various intermediates of the reaction are numbered **1**−**4**, and the possible products—HCN + HNO, HCN + HON, and H_2CO + N_2—are labeled **P1**, **P2,** and **P3**, respectively. **TS1**−**TS9** each denotes a transition species connecting to two intermediates located at local minima. The calculated geometric structures of local minima at the level B3LYP are shown in Figure 2, and the transition structures are shown in Figure 3. Pertinent aspects of the profiles of potential-energy surfaces (PES) calculated at the level CCSD(T) are shown in Figure 4. The calculated detailed energetic data with respect to the reactants **R** (H_2CN + NO) are listed in Table 2.

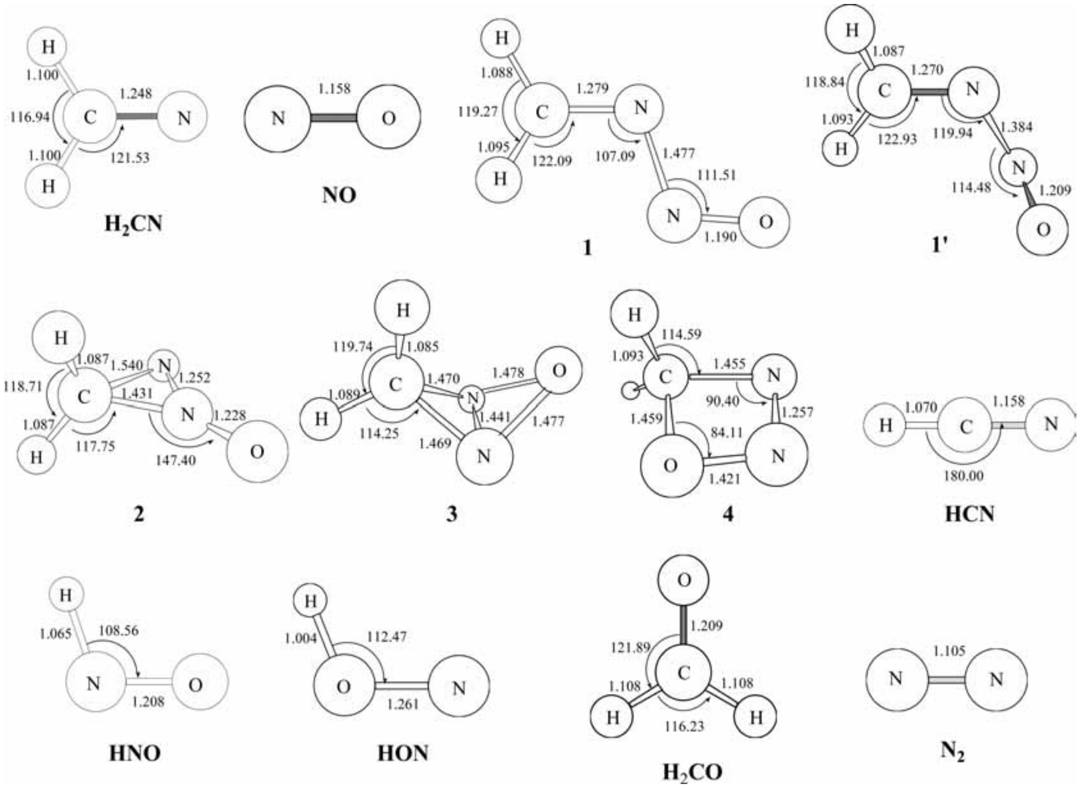

Figure 2. Optimized geometries of possible reactants, intermediates, and products on the potential-energy surface for the reaction of H_2CN with NO calculated at the level B3LYP/6-31++G(d,p); bond lengths are given in Å and angles in degrees.

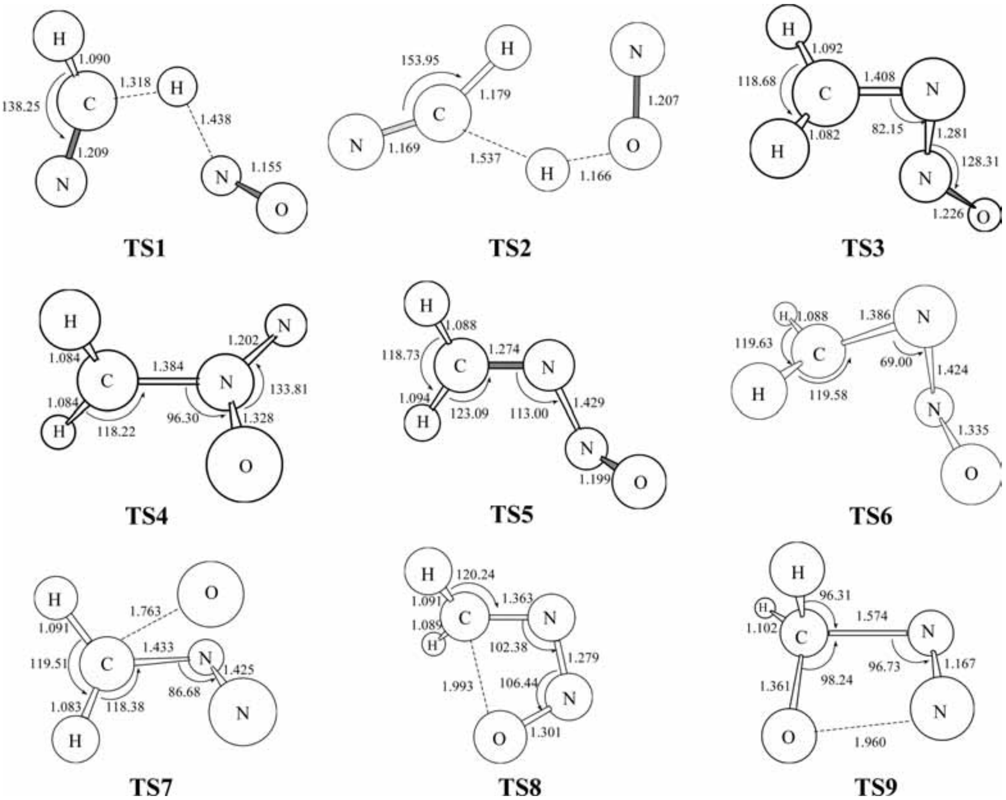

Figure 3. Optimized geometries of possible transition structures on the potential-energy surface for the reaction of H_2CN with NO calculated at the level B3LYP/6-31++G(d,p); bond lengths are given in Å and angles in degrees.

Comparing the calculated energetic data, we find that the formation of both products **P1** and **P3** are exothermic, whereas **P2** is endothermic about 20 kcal/mol. In addition, as shown in Figure 4, our calculated results for both channels **A** and **B** show that the barrier at **TS1** is 11.1 kcal/mol, much smaller than that of **TS2**, 19.9 kcal/mol. If H-abstraction would occur, channel **A** leading to **P1**, HCN + HNO, would thus be preferable to **B** with **P2**, HCN + HON. In the transition structures **TS1** and **TS2**, we found that the C···H bond length in the former is 1.318 Å, near that of the reactant H_2CN, 1.100 Å, whereas the C···H

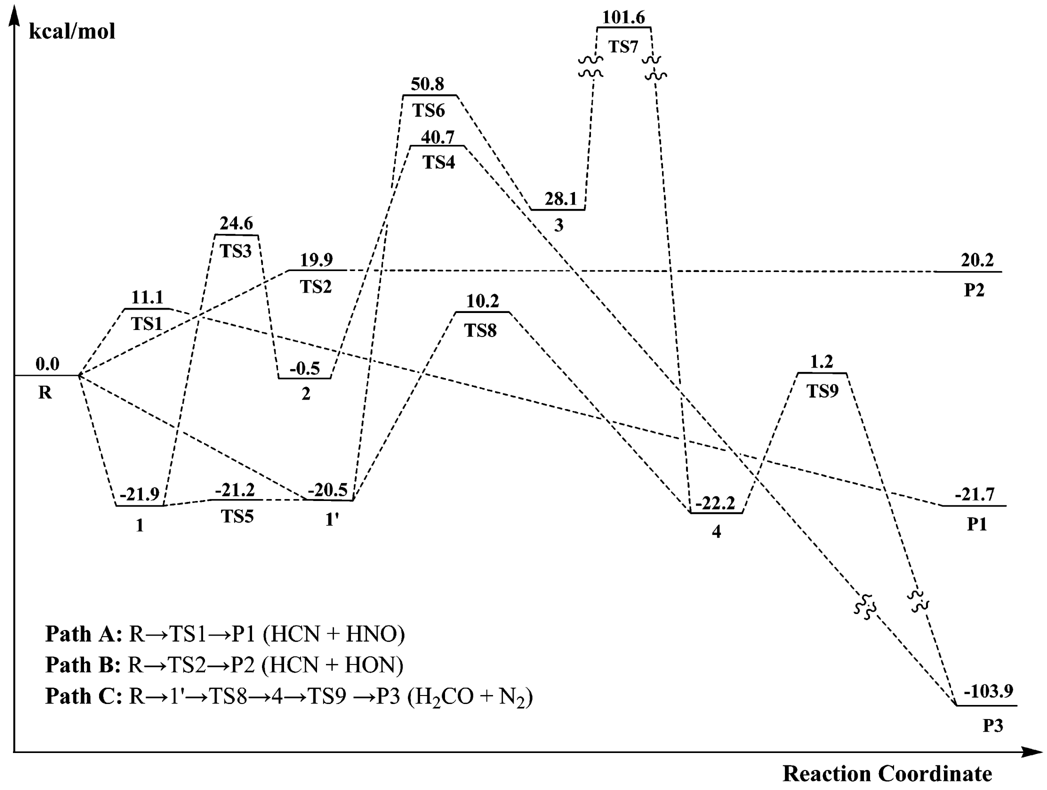

Figure 4. Calculated profiles on the potential-energy surface for possible pathways of the reaction of H_2CN with NO at the level CCSD(T)/aug-cc-PVTZ//B3LYP/6-31++G(d,p); the labels in the figure represent the same species as those in Figure 1.

TABLE 2: Zero-Point Vibration Energies (ZPE, hartree), Total Energies (TE, hartree), and Relative Energies (RE, kcal/mol) of Reactants, Intermediates, Transition States, and Products Calculated at the Level B3LYP/6-31++G(d,p) (BTE, BRE) and the Level CCSD(T)/aug-cc-PVTZ//B3LYP/6-31++G(d,p) (CTE, CRE) for the Systems of Both H_2CN and H_2SiN Plus NO

species	ZPE[a]	BTE+ZPE[b]	BRE[c]	CTE+ZPE[b]	CRE[c]
R (H_2CN+NO)	0.029765	−223.857778	0.0	−223.525918	0.0
1	0.036456	−223.888797	−19.5	−223.560860	−21.9
1′	0.036476	−223.888533	−19.3	−223.558525	−20.5
2	0.038655	−223.856599	0.7	−223.526744	−0.5
3	0.037251	−223.801558	35.3	−223.481062	28.1
4	0.038889	−223.885735	−17.5	−223.561270	−22.2
TS1	0.029348	−223.834048	14.9	−223.508267	11.1
TS2	0.028606	−223.820814	23.2	−223.494234	19.9
TS3	0.035844	−223.818691	24.5	−223.486786	24.6
TS4	0.034934	−223.785794	45.2	−223.461125	40.7
TS5	0.036062	−223.888394	−19.2	−223.559763	−21.2
TS6	0.033783	−223.765883	57.7	−223.444908	50.8
TS7	0.034059	−223.685128	108.3	−223.364032	101.6
TS8	0.036630	−223.838399	12.2	−223.509701	10.2
TS9	0.035315	−223.848083	6.1	−223.524073	1.2
P1 (HCN+HNO)	0.030278	−223.880553	−14.3	−223.560516	−21.7
P2 (HCN+HON)	0.029673	−223.817012	25.6	−223.493756	20.2
P3 (H_2CO+N_2)	0.032270	−224.009137	−95.0	−223.691468	−103.9
Rs (H_2SiN+NO)	0.021639	−475.209556	0.0	−474.514604	0.0
1's	0.026530	−475.277994	−42.9	−474.580561	−41.4
TS1s	0.022386	−475.169740	25.0	−474.481495	20.8
TS8s	0.026669	−475.273527	−40.1	−474.579336	−40.6
P1s (HSiN+HNO)	0.022964	−475.175590	21.3	−474.494156	12.8
P3s (H_2SiO+N_2)	0.024014	−475.414184	−128.4	−474.736355	−139.2

[a] Zero-point energy (au) at the level B3LYP/6-31++G(d,p). [b] The unit of energy is hartree. [c] Relative energy (kcal/mol) with respect to the reactants.

bond length in the latter was 1.537 Å, and O···H 1.166 Å, near that of the product HON 1.004 Å (in Figure 2). This result conforms with the Hammond postulate[53] that the former process, via **TS1**, would not only have a smaller energy barrier but also release more heat to attain the subsequent product.

The process of channel **C** involves first the formation of an adduct H_2CNNO, which has two isomers, *trans*-H_2CNNO (**1**) and *cis*-H_2CNNO (**1′**), with calculated energies 21.9 and 20.5 kcal/mol, respectively, below that of the reactants. Although the trans isomer is more stable than the cis by 1.4 kcal/mol, they might interconvert readily on overcoming a small barrier **TS5**, 0.7 kcal/mol. If the process begins from cis isomer adduct (**1′**), the preferable pathway would be **R** → **1′** → **TS8** → **4** → **TS9** → **P3** (channel **C**), as the highest energy of **TS8** along this pathway is only 10.2 kcal/mol above the reactant, compared to the other pathway **R** → **1′** → **TS6** → **3** → **TS7** → **4** → **TS9** → **P3** with the highest energy of **TS7** 101.6 kcal/mol above the reactant. There might be another pathway leading to the same **P3** product starting from the trans isomer adduct (**1**), **R** → **1** → **TS3** → **2** → **TS4** → **P3**, with the highest energy of **TS4** 40.7 kcal/mol above the reactant. Channel **C** is undoubtedly the most likely pathway regarding the **P3** formation. This favorable process, however, forms a cyclic intermediate, **4**, from the *cis*-H_2CNNO (**1′**) via a tight four-center transition structure (see **TS8** in Figure 3). In **TS8**, the C···O bond, 1.993 Å, is 0.534 Å longer than that in structure **4**, and it can readily decompose to $H_2CO + N_2$ with a barrier only 1.2 kcal/mol (**TS9**) above the reactants. This process is highly exothermic, −103.9 kcal/mol. In **TS9**, the C···O bond in the four-center ring structure is further shortened to 1.36 Å, and the N···O bond stretched to 1.96 Å, approaching the **P3** product. Our calculated results thus show the two major possible reaction pathways in H_2CN + NO to be channels **A** and **C**, with the latter thermochemically preferable.

Reaction H_2SiN + NO. The silicon-nitride related species—H_2SiN that is isovalent with H_2CN—is commonly applied to produce silicon nitride thin films used in microelectronics as well as protective coatings via chemical-vapor deposition (CVD)

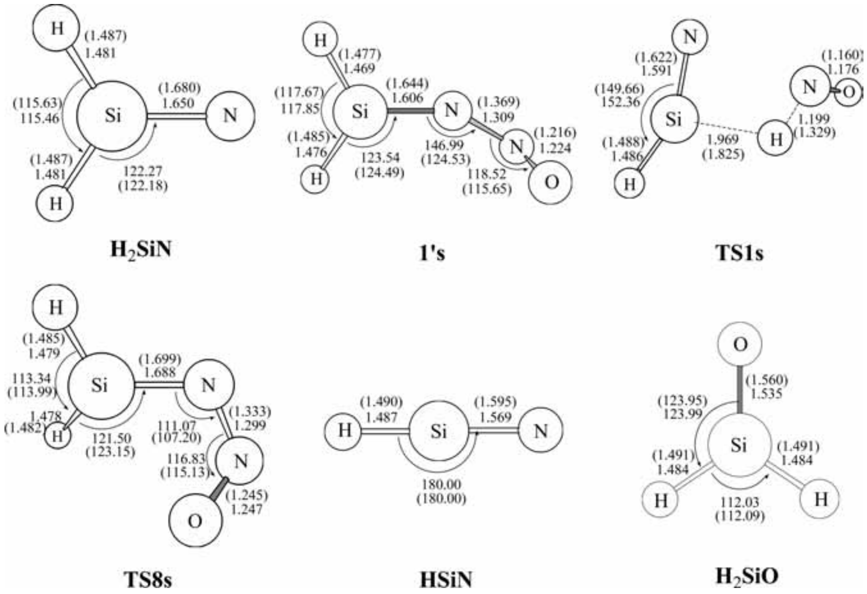

Figure 5. Optimized geometries of possible reactants, intermediates, transition structures, and products on the potential-energy surface for the reaction of H_2SiN with NO calculated at the level B3LYP/6-31++G(d,p). The numbers in parentheses are structural parameters calculated at the CCSD/aug-cc-PVDZ level. All bond lengths are given in Å and angles in degrees.

or plasma-assisted CVD processes, involving gaseous-phase reactions.[54−58] In a study of silicon-nitride derivatives, Melius et al.[59] made calculations on various Si−N species and gave geometries that can be compared with our results. For the molecule H_2SiN, they obtained bond lengths Si−H = 1.474 Å and Si−N = 1.667 Å (at the MP4(SDTQ) level); our calculated bond lengths optimized at the level B3LYP/6-31++G(d,p) are Si−H = 1.481 and Si−N = 1.650 Å, which agree satisfactorily. Our goal was to find other possible reactants, such as H_2SiN, that might replace the methylene amidogen radical (H_2CN), to react with NO and obtain lower barriers, especially along the similar pathway leading to the formation of gaseous N_2. According to a comparison of the energy barriers, we focused on analogous channels **A** and **C**, denoted as channels **As** and **Cs** for the reaction H_2SiN + NO. Our calculated geometric structures of stable reactants, intermediates, and transition states in the channels of **As** and **Cs** are drawn in Figure 5. The notation resembles that of the H_2CN counterparts except with addition of suffix ‘s’ to each symbol to represent the silicon-substituted species. The calculated energetic data with respect to reactants H_2SiN + NO are listed in the lower part of Table 2, and pertinent aspects of profiles on the potential-energy surface are presented in Figure 6. Channel **As**, **Rs** → **TS1s** → **P1s**, is a simple H-abstraction from H_2SiN to the N atom of NO to form **P1s**, HSiN + HNO, via transition state **TS1s**. The barrier of calculated transition state is large (**TS1s**), 20.8 kcal/mol, compared with the analogous pathway in H_2CN, 11.1 kcal/mol; it is also endothermic by 12.8 kcal/mol, in contrast to the exothermic H_2CN counterpart, −21.7 kcal/mol. All these facts indicate that it would take much greater effort to break the Si−H bond. Perhaps the empty d-orbital of the Si atom in H_2SiN strengthens the Si−H bonding. Our NBO[60] calculation shows large orbital coefficients of d_{yz} and d_{xz} between the Si−H bond, indicating the more pronounced d-character in H_2SiN, in agreement with this idea.

Channel Cs (**Rs** → **1’s** → **TS8s** → **P3s**). An adduct *cis*-H_2-SiNNO, **1’s**, was formed first and released much energy, −41.4 kcal/mol. The following reaction formed product **P3s**, H_2SiO + N_2, directly without forming any four-centered intermediate structure such as **4** in the case of H_2CN. Moreover, the only transition state in this pathway, **TS8s**, was also energetically more stable than the reactants by 40.6 kcal/mol, and the barrier from **1’s** to **TS8s** was almost zero—only 0.8 kcal/mol, leading to a stable product **P3s**, highly exothermic at −139.2 kcal/mol. To evaluate the accuracy of the calculated relative energies we also applied optimization calculations at the CCSD/aug-cc-PVDZ level (more effective electron correlation) as well as G2 and G3 levels specifically for these important species (Rs, **1’s**, TS1s, TS8s, P1s, and P3s). The result is quite consistent in these levels except that the relative energies of CCSD data all upshift about 10 kcal/mol as compared to other levels, shown in Table 3.

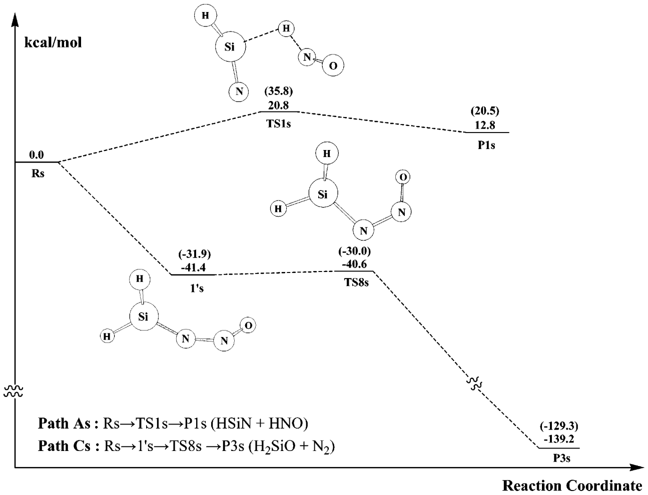

Figure 6. Calculated profiles on the potential-energy surface for two major pathways of the reaction of H_2SiN with NO at the level CCSD-(T)/aug-cc-PVTZ// B3LYP/6-31++G(d,p). The number in parentheses is from CCSD/aug-cc-PVDZ.

The major difference between H_2CN and H_2SiN toward NO warrants scrutiny. First, comparing the relative stability in forming the adducts **1′** and **1’s**, we found that the latter is more stable than the former by 20.9 kcal/mol. We calculated the Fukui functions[61] and applied the theory of hard-and-soft acid-and-base (HSAB) to seek possible clues. The HSAB principle has been useful to explain the behavior of many chemical systems.[62−65] The extrapolation locally of a general behavior “soft likes soft” and “hard likes hard”, together with an idea

TABLE 3: Total (Including ZPE, au) and Relative Energies (RE, kcal/mol) of Reactant, Intermediates, Transition States, and Products for $H_2SiN + NO$ Calculated at Different Levels of Theory

	energies						
species	RE(CCSD(T)−sp)[a]	CCSD/aug-cc-PVDZ	RE(CCSD)[b]	G2	RE(G2)[c]	G3	RE(G3)[d]
Rs ($H_2SiN+NO$)	0.00	−474.313060	0.00	−474.552443	0.00	−474.984510	0.00
1’s	−41.39	−474.363912	−31.91	−474.621235	−43.17	−475.050204	−41.22
TS1s	20.78	−474.256043	35.78	−474.519522	20.66	−474.949321	22.08
TS8s	−40.62	−474.360880	−30.01	−474.619062	−41.80	−475.047800	−39.72
P1s ($HSiN+HNO$)	12.83	−474.280445	20.47	−474.530161	13.98	−474.959956	15.41
P3s (H_2SiO+N_2)	−139.15	−474.519035	−129.25	−474.772298	−137.96	−475.203533	−137.44

[a] The relative energy with respect to reactants at the CCSD(T)/aug-cc-PVTZ//B3LYP/6-31++g(d,p) level. [b] The relative energy with respect to reactants at the CCSD/aug-cc-PVDZ level. [c] The relative energy with respect to reactants at the G2 level. [d] The relative energy with respect to reactants at the G3 level.

TABLE 4: Condensed Fukui Functions for the H and N Atoms in H_2CN and H_2SiN Radicals and the N Atom in NO as Well as the Global and Local Softnesses of the Molecules Calculated at the Level B3LYP/6-31++G(d,p)

	f^{0} [a]			local softness (s^0)[c]	
molecule	H	N	global softness S[b]	H	N
NO		0.612	2.998		1.834
H_2CN	0.204	0.188	3.286	0.670	0.616
H_2SiN	0.143	0.563	2.185	0.313	1.230

[a] Atomic charges according to a natural population analysis (NPA). [b] $S = 1/(\text{IE-EA})$, IE is the ionization energy, and EA is the electron affinity; the energy unit is hartree. [c] $s^0 = f^{\,0}\cdot S$.

that the larger is the value of the Fukui function, the greater is the reactivity, is also a useful approach to explain the chemical reactivity of diverse systems.[66] We chose the $f^{\,0}$ value for comparison because our title reactions are more characteristic of a radical reaction.[67] In their derivation of the equation of interaction energy in terms of the local softness and the condensed Fukui function of an atom in the molecule, Ga’zquez et al.[61] pointed out that the largest value of the Fukui function is, in general, associated with the most reactive site. According to our calculated data in Table 4, the calculated Fukui function ($f^{\,0}$) 0.563 of the N atom in the H_2SiN radical is clearly nearer 0.612 for the N atom in NO than the value 0.188 of the N atom in the H_2CN radical, which accounts for the formation of the adduct *cis*-H_2SiNNO **1’s** being more preferable than that of the adduct *cis*-H_2CNNO **1′**. Applying the HSAB theory, we find in contrast that the difference of the local softness (s^0) 1.230 of the N atom in H_2SiN and 1.834 of the N atom in NO is smaller than that of 0.616 of the N atom in H_2CN and 1.834 of the N atom in NO, which also accounts for the favorable formation of the adduct *cis*-H_2SiNNO **1’s**. We employ a similar approach to explain the barrier difference between **TS1** and **TS1s** in the H-abstraction pathways. The calculated Fukui functions ($f^{\,0}$) of the H atom in H_2CN and the N atom in the NO radical are closer than those in the counterparts $H_2SiN + NO$. This approach is thus also applicable to explain the energy preference of **TS1** over **TS1s**.

The uniquely strong interaction of the channel **Cs** pathway in the reaction $H_2SiN + NO$ is surprising and needs to be understood. Our NBO calculation shows a strong secondary interaction, $E_2 = 70.95$ kcal/mol, between the lone pair electrons of the N atom and the antibonding orbital σ^*_{N-O} in the adduct structure *cis*-H_2SiNNO **1’s**, whereas a similar interaction is much smaller in its counterpart of the adduct *cis*-H_2CNNO, **1′**, $E_2 = 19.87$ kcal/mol. This factor might contribute some stability for **1’s** being more stable than **1′**. Moreover, a four-membered ring structure **4** is an essential intermediate before leading to **P3** in the channel **C** pathway of the reaction $H_2CN + NO$. The formation of **4** from **1′** requires a large barrier, 30.7 kcal/mol, for **1′** → **TS8** → **4**, because the structure of **1′** is far from the nearly square four-membered ring structure **4**, so that the ∠CNN angle of **1′** must twist from 119.94° to 102.38° (**TS8**) and the dihedral angle of ∠CNNO from −94.43° to −20.05° (**TS8**); the most important part is to lengthen the C−N bond from 1.270 to 1.363 Å, which requires energy. The NBO result shows also a strong secondary interaction between the σ_{C-O} and σ^*_{N-N} orbitals, which further stabilizes the structure **TS8**. In contrast, no similar four-membered ring intermediate is found after **1’s**, and it leads to **P3s** directly. The only found transition structure **TS8s** differs little from **1’s** (especially the Si−N bond distance), and it is further stabilized by a moderately strong secondary interaction between the σ_{Si-N} and σ^*_{N-O} orbitals, not found in the **TS8** counterpart. All these effects account for the small increase of energy, 0.8 kcal/mol, from **1’s** to **TS8s**. The absence of a four-membered ring intermediate in the channel **Cs** pathway also indicates that there exists a strong interaction between Si

TABLE 5: Nominal Properties of Transition States in the Systems H_2CN and H_2SiN Plus NO at the B3LYP/6-31++G Level**

species	vibrational wavenumbers/cm^{-1}	principal moments of inertia (amu $bohr^2$)
TS1	1112i,170, 311, 377, 631, 705, 1090, 1134, 1496, 1885, 1916, 3169	61.7, 393.5, 421.9
TS2	715i, 194, 232, 422, 818, 997, 1038, 1219, 1520, 1767, 1991, 2359	43.8, 508.7, 552.5
TS3	816i, 351, 612, 792, 959, 1083, 1121, 1295, 1514, 1629, 3112, 3266	49.1, 269.1, 301.6
TS4	616i, 454, 479, 514, 911, 1001, 1095, 1192, 1454, 1744, 3171, 3321	123.2, 163.4, 273.6
TS5	110i, 346, 522, 664, 895, 1077, 1188, 1472, 1653, 1720, 3083, 3209	38.6, 323.8, 335.7
TS6	845i, 432, 550, 656, 899, 980, 1067, 1186, 1273, 1453, 3110, 3224	79.5, 199.3, 215.3
TS7	940i, 527, 678, 748, 847, 875, 1050, 1136, 1236, 1513, 3086, 3255	114.1, 147.0, 182.9
TS8	739i, 547, 771, 976, 1009, 1146, 1165, 1229, 1371, 1530, 3114, 3221	95.4, 158.6, 241.1
TS9	1046i, 386, 477, 713, 1014, 1089, 1146, 1258, 1514, 1883, 2984, 3037	94.0, 174.8, 254.0
TS1s	301i, 141, 222, 242, 283, 432, 619, 1145, 1225, 1477, 1828, 2211	114.5, 573.8, 645.5
TS1s[a]	1100i, 177, 217, 255, 300, 432, 469, 1061, 1088, 1318, 1825, 2247	115.9, 536.7, 611.6
TS8s	194i, 307, 412, 520, 632, 827, 864, 990, 1187, 1407, 2260, 2299	105.9, 354.4, 443.5
TS8s[a]	253i, 355, 395, 575, 635, 827, 883, 981, 1105, 1415, 2271, 2303	111.3, 338.7, 433.2

[a] At the CCSD/aug-cc-PVDZ level.

and O atoms that pulls these two atoms together and forms $H_2SiO + N_2$ directly, concurrently releasing much heat. The empty d orbital in Si atom is believed to play an important role in this strong interaction, which is a unique property that the carbon atom lacks in the reaction $H_2CN + NO$.

Conclusion

From the calculated potential energy surfaces, we predict that the preferable product formation in the $H_2CN + NO$ reaction could be P1 and P3 (with similar energy barrier around 11 kcal/mol), yet P3 is thermodynamically much favorable. On the other hand, in the replacement of H_2CN with H_2SiN toward the reaction with NO the most probable reaction pathway became the one that reduced NO to N_2 molecule via a barrierless process (path Cs). We also applied the TST (transition state theory) method to calculate the rate constants of the proposed two channels (path As and Cs) in the reaction of $H_2SiN + NO$ under 298 K. The potential energy surface was calculated both at the CCSD(T) level and the G2 level, and the results do not differ too much. The rate constant of pathway As (at G2 level) leading to P1s (HSiN + HNO) is 1.37×10^{-9}, compared to pathway Cs leading to P3s ($H_2SiO + N_2$), 5.95×10^{35}; while that of CCSD(T) is 2.41×10^{-10} and 3.64×10^{34} (cm^3 $molecule^{-1}$ s^{-1}), respectively. Since there are no experimental data to compare with, these data can be considered as a rough estimation according to TST. The result of this study will be of great value in searching for the effective reagents of converting the industrial pollutants containing toxic NO into stable and harmless nitrogen gases, and this discovery of the reaction pathway for $H_2SiN + NO$ might be useful for studies of thermal $DeNO_x$.

Acknowledgment. We are grateful to the National Science Council of Republic of China (NSC 94-2113-M-003-005) for the funding of this research and to the National Center for High-Performance Computing for providing the Gaussian package and computer time. We also want to thank Prof. M. Hayashi and Prof. J. C. Jiang for their useful discussion about the appropriate rate constant calculation in this manuscript.

Appendix

We provide calculated wavenumbers and moments of inertia for each transition structure from **TS1** to **TS9** (H_2CN plus NO) and for **TS1s** and **TS8s** (H_2SiN plus NO) (see Table 5).

References and Notes

(1) Cochran, E. L.; Adrian, F. J.; Bowers, V. A. *J. Chem. Phys*. **1962**, *36*, 1938.

(2) Marston, G.; Stief, L. J. *Res. Chem. Intermed*. **1989**, *12*, 161.

(3) Marston, G.; Nesbitt, F. L.; Stief, L. J. *J. Chem. Phys*. **1989**, *91*, 3483.

(4) Nesbitt, F. L.; Marston, G.; Stief, L. J.; Wickramaaratchi, M. A.; Tao, W.; Klemm, R. B. *J. Phys. Chem*. **1991**, *95*, 7613.

(5) Ohishi, M.; McGonagle, D.; Irvine, W. M.; Yamamoto, S.; Saito, S. *Astrophys. J.* **1994**, *427*, L51.

(6) Alexander, M. H.; Dagdigian, P. J.; Jacox, M. E.; Kolb, C. E.; Melius, C. F. *Prog. Energy Combust. Sci.* **1991**, *17*, 263.

(7) Adams, G. F.; Shaw, R. W., Jr. *Annu. Rev. Phys. Chem.* **1992**, *43*, 311.

(8) Zhao, X.; Hintsa, E. J.; Lee, Y. T. *J. Chem. Phys.* **1988**, *88*, 801.

(9) Melius, C. F. Thermochemical Modeling: II. Application to Ignition and Combustion of Energetic Materials. *Chemistry and Physics of Energetic Materials*; Bulusu, S. N., Ed.; 1990; pp 51−78.

(10) Marston, G.; Nesbitt, F. L.; Nava, D. F.; Payne, W. A.; Steif, L. J. *J. Phys. Chem.* **1989**, *93*, 5769.

(11) Miller, J. A.; Melius, C. F.; Glarborg, P. *Int. J. Chem. Kinet.* **1998**, *30*, 223.

(12) Lebonnois, S.; Toublanc, D.; Houdin, F.; Rannou, P. *Icarus* **2001**, *152*, 384.

(13) Kimball-Linne, M. A.; Hanson, R. K. *Combust. Flame* **1986**, *64*, 337.

(14) Lyon, R. K.; Hardy, J. E. *Ind. Eng. Chem. Fundam*. **1986**, *25*, 19.

(15) Lyon, R. K. *194th Ann. ACS Meet.; Div. Fuel Chem.* **1987**, *32*, 433.

(16) Glarborg, P.; Dam-Johansen, K.; Miller, J. A.; Kee, R. J.; Coltrin, M. E. *Int. J. Chem. Kinet.* **1994**, *26*, 421.

(17) Miller, J. A.; Glarborg, P. *Springer Ser. Chem. Phys*. **1996**, *61*, 318.

(18) Lyon, R. K. U.S. Patent 3, 900, 559, 1975.

(19) Lyon, R. K. *Environ. Sci. Technol.* **1987**, *21*, 231−236.

(20) Miller, J. A.; Klippenstein, S. J. *J. Phys. Chem. A* **2000**, *104*, 2061.

(21) Misono, M.; Hirao, Y.; Yokoyama, C. *Catal. Today* **1997**, *38*, 157.

(22) Hayhurst, A. N.; Lawrence, A. D. *Combust. Flame* **1997**, *110*, 351.

(23) Honkala, K.; Pirila, P.; Laasonen, K. *Surf. Sci.* **2001**, *489*, 72.

(24) Smits, R.; Iwasawa, Y. *Appl. Catal. B* **1995**, *6*, 201.

(25) Suzuki, S.; Moriyama, H.; Murata. K. *Energy Fuels* **2002**, *16*, 1173.

(26) Schmidt, C.; Sowade, T.; Loffler, E.; Birkner, A.; Grunert, W. *J. Phys. Chem. B* **2002**, *106*, 4085.

(27) Parvulescu, V. I.; Grange, P.; Delmon, B. *Catal. Today* **1998**, *46*, 233.

(28) Traa, Y.; Burger, B.; Weitkamp, J. *Microporous Mesoporous Mater*. **1999**, *30*, 3.

(29) Bennici, S.; Gervasini, A.; Ravasio, N.; Zaccheria, F. *J. Phys. Chem. B* **2003**, *107*, 5168.

(30) Yeom, Y. H.; Wen, B.; Sachtler, W. M. H.; Weitz, E. *J. Phys. Chem. B* **2004**, *108*, 5386.

(31) Cooper, W. F.; Park, J.; Hershberger, J. F. *J. Phys. Chem.* **1993**, *97*, 3283.

(32) Baren, R. E.; Hershberger, J. F. *J. Phys. Chem. A* **2002**, *106*, 11093.

(33) Thweatt, W. D.; Erickson, M. A.; Hershberger, J. F. *J. Phys. Chem. A* **2004**, *108*, 74.

(34) Rim, K. T.; Hershberger, J. F. *J. Phys. Chem. A* **2004**, *104*, 293.

(35) Meyer, J. P.; Hershberger, J. F. *J. Phys. Chem. A* **2005**, *109*, 4772.

(36) Jursic, B. S. *J. Phys. Chem. A* **1999**, *103*, 1880.

(37) Jursic, B. S. *J. Phys. Chem. A* **2000**, *104*, 1363.

(38) (a) Rongshun, Z.; Lin, M. C. *J. Phys. Chem. A* **2000**, *104*, 10807. (b) Tokmakov, I. V.; Moskaleva, L. V.; Paschenko, D. V.; Lin, M. C. *J. Phys. Chem. A* **2003**, *107*, 1066.

(39) Chen, H.-T.; Ho, J.-J. *J. Phys. Chem. A* **2005**, *109*, 2564.

(40) (a) Liu, J.-J.; Ding, Y.-H.; Feng, J.-K.; and Sun, C.-C. *J. Phys. Chem. A* **2001**, *105*, 9901. (b) Tao, Y.-G.; Ding, Y.-H.; Li, Z.-S.; Huang, X.-R.; Sun, C.-C. *J. Phys. Chem. A* **2001**, *105*, 3388.

(41) (a) Keefer, L. K.; Nims, R. W.; Davies, K. M.; Wink, D. A. *Methods Enzymol*. **1996**, *268*, 281. (b) Hrabie, J. A.; Srinivasan, A.; George, C.; Keefer, L. K. *Tetrahedron Lett.* **1998**, *39*, 5933. (c) Hrabie, J. A.; Arnold, E. V.; Citro, M. L.; George, C.; Keefer, L. K. *J. Org. Chem*. **2000**, *65*, 5745.

(42) (a) Hrabie, J. A.; Keefer, L. K. *Chem. Rev*. **2002**, *102*, 1135. (b) Arnold, E. V.; Citro, M. L.; Keefer, L. K.; Hrabie, J. A. *Org. Lett*. **2002**, *4*, 1323. (c) Hrabie, J. A.; Citro, M. L.; Chmurny, G. N.; Keefer, L. K. *J. Org. Chem*. **2005**, *70*, 7647.

(43) Frisch, M. J.; Trucks, G. W.; Schlegel, H. B.; Scuseria, G. E.; Robb, M. A.; Cheeseman, J. R.; Montgomery, J. A., Jr.; Vreven, T.; Kudin, K. N.; Burant, J. C.; Millam, J. M.; Iyengar, S. S.; Tomasi, J.; Barone, V.; Mennucci, B.; Cossi, M.; Scalmani, G.; Rega, N.; Petersson, G. A.; Nakatsuji, H.; Hada, M.; Ehara, M.; Toyota, K.; Fukuda, R.; Hasegawa, J.; Ishida, M.; Nakajima, T.; Honda, Y.; Kitao, O.; Nakai, H.; Klene, M.; Li, X.; Knox, J. E.; Hratchian, H. P.; Cross, J. B.; Bakken, V.; Adamo, C.; Jaramillo, J.; Gomperts, R.; Stratmann, R. E.; Yazyev, O.; Austin, A. J.; Cammi, R.; Pomelli, C.; Ochterski, J. W.; Ayala, P. Y.; Morokuma, K.; Voth, G. A.; Salvador, P.; Dannenberg, J. J.; Zakrzewski, V. G.; Dapprich, S.; Daniels, A. D.; Strain, M. C.; Farkas, O.; Malick, D. K.; Rabuck, A. D.; Raghavachari, K.; Foresman, J. B.; Ortiz, J. V.; Cui, Q.; Baboul, A. G.; Clifford, S.; Cioslowski, J.; Stefanov, B. B.; Liu, G.; Liashenko, A.; Piskorz, P.; Komaromi, I.; Martin, R. L.; Fox, D. J.; Keith, T.; Al-Laham, M. A.; Peng, C. Y.; Nanayakkara, A.; Challacombe, M.; Gill, P. M. W.; Johnson, B.; Chen, W.; Wong, M. W.; Gonzalez, C.; Pople, J. A. *Gaussian 03, revision C.02*; Gaussian, Inc.: Wallingford, CT, 2004.

(44) (a) Becke, A. D. *J. Chem. Phys*. **1993**, *98*, 5648. (b) Becke, A. D. *J. Chem. Phys*. **1992**, *96*, 2155. (c) Becke, A. D. *J. Chem. Phys*. **1992**, *97*, 9173.

(45) Lee, C.; Yang, W.; Parr, R. G. *Phys. Rev.* **1988**, *B37*, 785.

(46) Gonzalez, C.; Schlegel, H. B. *J. Phys. Chem.* **1989**, *90*, 2154.

(47) Lee, T. J.; Scuseria, G. In *Quantum-mechanical Electronic Structure Calculations with Chemical Accuracy*; Langhoff, S. F., Ed.; Kluwer Academic Press: Dordrecht, The Netherlands, 1995.

(48) Knowles, P. J.; Hampel, C.; Werner, H.-J. *J. Chem. Phys*. **1993**, *99*, 5219.

(49) Yamamoto, S.; Saito, S. *J. Chem. Phys*. **1992**, *96*, 4157.

(50) Berkowitz, J.; Ellison, G. B.; Gutman, D. *J. Phys. Chem.* **1994**, *98*, 2744.

(51) Kuo, S.-C.; Zhang, Z.; Ross, S. K.; Klemm, R. B. *J. Phys. Chem. A* **1997**, *101*, 4035.

(52) Drury-Lessard, C. R.; Moule, D. C. *Chem. Phys. Lett.* **1977**, *47*, 300.

(53) Hammond, G. S. *J. Am. Chem. Soc.* **1955**, *77*, 334.

(54) See, for example: Ho, P.; Buss, R. J.; Loehman, R. E. *J. Mater. Res.* **1989**, *4*, 873 and references therein.

(55) Kapoor, V. J.; Stein, H. J. *Silicon Nitride Thin Insulating Films*; Symposium Proceedings; The Electrochemical Society, Inc.: Pennington, NJ, 1983; Vol. 83−8.

(56) Belyi, V. I.; Vasilyeva, L. L.; Ginovker, A. S.; Gritsenko, V. A.; Repinsky, S. M.: Sinitsa, S. P.; Smirnova, T. P.; Edelman, F. L. *Silicon Nitride in Electronics*; Materials Science Monographs; Elsevier: Amsterdam, 1988; Vol 34.

(57) Galasso, F. S.; Veltri, R. D.; Croft, W. J. *Am. Ceram. Soc. Bull.* **1978**, *57*. 453.

(58) Gebhardt, J. J.; Tanzilli, R. A.; Harris, T. A. *J. Electrochem. Soc.* **1976,** *123*, 1578.

(59) Melius, C. F.; Ho, P. *J. Phys. Chem.* **1991**, *95*, 1410.

(60) Glendering, E. D.; Reed, A. E.; Carpenter, J. E.; Weinhold, F. *NBO, ver. 3.1*; Gaussian. Inc.: Pittsburgh, PA, 1998.

(61) Ga’zquez, J. L.; Men’dez, F. *J. Phys. Chem.* **1994**, *98*, 4591.

(62) Roy, R. S.; Gehring, A. M.; Milne, J. C.; Belshaw, P. J.; Walsh, C. T. *Nat. Prod. Rep.* **1999**, *16*, 249.

(63) (a) Gordon, M. D.; Alston, P. V.; Rossi, A. R. *J. Am. Chem. Soc.* **1978**, *100*, 5701. (b) Nguyen, L. T.; Proft, F. D.; Chandra, A. K.; Uchimaru, T.; Nguyen, M. T.; Geerlings, P. *J. Org. Chem.* **2001**, *66*, 6096. (c) Nguyen, M. T.; Chandra, A. K.; Sakai, S.; Morokuma, K. *J. Org. Chem.* **1999**, *64*, 65.

(64) El-Bakali Kassimi, N.; Doerksen, R. J.; Thakkar, A. J. *J. Phys. Chem.* **1996**, *100*, 8752.

(65) (a) Langenaeker, W.; Demel, K.; Geerlings, P. *J. Mol. Struct.: THEOCHEM* **1992**, *259*, 317. (b) Langenaeker, W.; Demel, K.; Geerlings, P. *J. Mol. Struct.: THEOCHEM* **1991**, *234*, 329.

(66) Parr, R. G.; Yang, W. *Annu. Rev. Phys. Chem.* **1995**, *46*, 701.

(67) Yang, W.; Mortier, W. J. *J. Am. Chem. Soc.* **1986**, *108*, 5708.